Analysis of epidemic spreading of an SIRS model in complex heterogeneous networks

Chun-Hsien Li[1], **Chiung-Chiou Tsai**[2] and Suh-Yuh Yang[3]

Abstract

In this paper, we study the spreading of infections in complex heterogeneous networks based on an SIRS epidemic model with birth and death rates. We find that the dynamics of the network-based SIRS model is completely determined by a threshold value. If the value is less than or equal to one, then the disease-free equilibrium is globally attractive and the disease dies out. Otherwise, the disease-free equilibrium becomes unstable and in the meantime there exists uniquely an endemic equilibrium which is globally asymptotically stable. A series of numerical experiments are given to illustrate the theoretical results. We also consider the SIRS model in the clustered scale-free networks to examine the effect of network community structure on the epidemic dynamics.

Keywords: epidemic model; complex network; community structure; Lyapunov function; global stability.

AMS subject classifications: 92D30; 34D23; 37B25; 05C82.

Running title: Epidemic spreading in complex heterogeneous networks.

1. Introduction

The mathematical modeling of infectious disease spreading has been extensively studied for a long time; see [5] and many references cited therein. For better understanding the spreading dynamics, a lot of epidemic models have been developed and analyzed. One kind of such models is the so-called compartmental models which are composed of ordinary differential equations (ODEs) [5, 7, 11, 22]. In this kind of approach, the entire population are divided into different compartments and each compartment corresponds to an epidemiological state which depends on the characteristics of the particular disease being modeled. In general, the underlying assumption for compartmental models is that the population size is large enough such that the mixing of individuals is homogeneous. However, it has been observed that in reality, there exist some members, called super-spreaders, who could transmit infection to many other members of the population [19]. Thus, the homogeneous mixing hypothesis may not be appropriate when the effect of contact heterogeneity is incorporated

[1] Department of Mathematics, National Kaohsiung Normal University, Yanchao District, Kaohsiung City 82444, Taiwan. E-mail: chli@nknucc.nknu.edu.tw.
[2] Department of Computer Science and Information Engineering, Taoyuan Innovation Institute of Technology, Jhongli City, Taoyuan County 32091, Taiwan. E-mail: cctsai@tiit.edu.tw.
[3] Department of Mathematics, National Central University, Jhongli City, Taoyuan County 32001, Taiwan. E-mail: syyang@math.ncu.edu.tw. Tel.: +886-3-4227151 ext. 65130; fax: +886-34257379.

into the compartmental models.

To deal with the effect of contact heterogeneity, the disease transmission should be modeled over complex heterogeneous networks. In a complex network, each node represents an individual in its corresponding epidemiological state, and each edge between two nodes stands for an interaction that may allow disease transmission. In recent years, considerable concern has arisen over the heterogeneity in human contact patterns in epidemic spreading research. Several network-based approaches have been developed to model such complex patterns of interactions. We refer the reader to, e.g., [3, 4, 6, 9, 10, 12, 15, 17, 18, 20, 21, 23, 24, 25, 26, 27, 28, 29, 30]. One of the pioneer works in this area was introduced by Pastor-Satorras and Vespignani [17, 18]. They studied the SIS model in scale-free networks [2] and showed that the spread of infections is tremendously strengthened on scale-free networks. Also, the SIR model in complex networks was studied in [12], and it is indicated that the connectivity fluctuations of the network play a major role by strongly enhancing the incidence of infection.

It is worth noting that the above-mentioned studies [17, 18] figured out that there exists an epidemic threshold so that if the effective spreading rate is above this threshold, then the infection can produce an epidemic outbreak. However, to the best of our knowledge, there is not a mathematically rigorous proof for such significant results until the seminal paper of Wang and Dai [20]. They proved that if the effective spreading rate is above the epidemic threshold, then as long as there exist infected nodes in the network initially, infections will spread and eventually approach a unique positive equilibrium of the network-based SIS model. Very recently, in [29], the authors proposed a new network-based SIS model with nonlinear infectivity as well as birth and death rates. The basic reproductive number R_0 (cf. [1]) was established and it was shown that if $R_0 \le 1$, then the disease-free equilibrium is globally attractive. Otherwise, the positive epidemic equilibrium is globally attractive. Moreover, the authors also studied a generalized epidemic model on complex heterogeneous networks in [30]. Besides, an SEIRS model with infectivity assumed to be either constant or proportional to the node degree in scale-free networks was presented in [10], in which the local stability analysis of the disease-free equilibrium and the permanence of the disease in the network were provided.

As we have seen in the literature, the most important issues for studying the epidemic models in mathematical epidemiology are the stability and permanence. For the traditional compartment models, many advances have been made in this direction; see e.g., [5, 7, 22] and many references cited therein. However, to date, there has been relatively little research conducted on network-based epidemic models [10, 16, 20, 21, 23, 25, 27, 28, 29, 30]. The main purpose of this paper is to study the global dynamics of a newly proposed SIRS network-based model with birth and death rates as well as nonlinear infectivity. We first establish the new epidemic threshold R_0, see (2.2) below, which determines the existence of the positive endemic equilibrium. We then prove that if the

threshold value $R_0 \le 1$, the disease-free equilibrium is globally attractive. Moreover, it is indeed globally asymptotically stable provided $R_0 < 1$. Otherwise, if $R_0 > 1$ then the disease-free equilibrium is unstable and at the same time, there exists uniquely a positive endemic equilibrium which is globally asymptotically stable.

In this paper, we perform numerical experiments of several illustrative examples with a finite size of scale-free network to support the theoretical analysis. Since it has been pointed out that the social networks has community structure [9, 13, 14], we further consider the SIRS model in the so-called clustered scale-free networks, that is, within which each cluster is a scale-free subnetwork, to examine the effect of network community structure on the epidemic dynamics. In our numerical experiments, we find that for the convergence of disease-free steady state, the larger the degree of community is, the faster the convergence will be. On the other hand, for the convergence of endemic steady state, the larger the degree of community is, the stronger the density of susceptible nodes will be and, in contrast, the weaker the densities of infected and recovered nodes are.

The rest of this paper is organized as follows. In Section 2, we propose a network-based SIRS epidemic model with birth and death rates. We then discuss the positivity and boundedness of solutions of the SIRS epidemic system. In Section 3, we study the global stability of the disease-free and endemic equilibria. In Section 4, a series of numerical experiments are given to illustrate the theoretical results. Finally, conclusions and future works are drawn in Section 5.

2. Network-based SIRS model

In this section, we will propose a network-based SIRS epidemic model with birth and death rates. First, we classify all the nodes in the given network into n groups such that the nodes in the same group have the same connectivity (i.e., the same degree). That is, each node in the *i*-th group has the same connectivity, say k_i, for i =1, 2, ⋯ ,*n*. In addition, according to the spreading of SIRS process, each node could have one of the three epidemiological states: susceptible, infected, or recovered. Therefore, we let $S_{k_i}(t)$, $I_{k_i}(t)$ and $R_{k_i}(t)$ be the densities of susceptible, infected and recovered nodes of the *i*-th group at time t, respectively, and let $N_{k_i}(t) = S_{k_i}(t) + I_{k_i}(t) + R_{k_i}(t)$ for all $t \ge 0$ and i =1, 2, ⋯ ,*n*. With these notations, the dynamics of the network-based SIRS model can be described by the following system of ODEs:

$$\begin{cases} S'_{k_i}(t) = bN_{k_i}(t) - \lambda(k_i)S_{k_i}(t)\Theta(t) - \mu S_{k_i}(t) + \gamma R_{k_i}(t) \\ I'_{k_i}(t) = \lambda(k_i)S_{k_i}(t)\Theta(t) - \alpha I_{k_i}(t) - \mu I_{k_i}(t) \\ R'_{k_i}(t) = \alpha I_{k_i}(t) - \mu I_{k_i}(t) - \gamma R_{k_i}(t) \end{cases} \qquad i = 1, 2, \cdots, n,\ t > 0 \quad (2.1)$$

where $\lambda(k_i) > 0$ is the degree-dependent infection rate; the natural births and deaths are

proportional to the density of nodes with birth rate $b > 0$ and death rate $\mu > 0$; $\alpha > 0$ is the recovery rate of the infected nodes; $\gamma > 0$ is the average loss of immunity rate. The dynamics of n groups of SIRS subsystems are coupled through the function $\Theta(t)$, which is the proportion of infective occupied edges over the entire network given by

$$\Theta(t) = \frac{1}{\langle k \rangle} \sum_{j=1}^{n} \varphi(k_j) P(k_j) I_{k_j}(t)$$

where $P(k_j) > 0$ is the probability that a node has degree k_j and thus $\sum_{j=1}^{n} P(k_j) = 1$; $\langle k \rangle \sum_{j=1}^{n} k_j P(k_j)$ denotes the mean degree; $\varphi(k_j)$ denotes the infectivity of a node with degree k_j. It should be noticed that various types of the infectivity $\varphi(k_j)$ have been considered. For instance, the simplest type is constant infectivity $\varphi(k_j) = C$ [10, 24], the second type is given as $\varphi(k_j) = k_j$ [9, 12, 17, 18, 20], the third type takes the form $\varphi(k_j) = k_j T(k_j)$ [15] with probability $T(k_j)$ that an infected node would actually admit an infection through an edge connected to a susceptible node. Besides, a nonlinear infectivity $\varphi(k_j) = \rho k_j^a / (1 + \nu k_j^a)$ was concerned in [26, 29]. We will consider various infectivities in the numerical experiments in Section 4.

Throughout this paper, we need the following assumptions: (i) the infection rate is assumed to be bounded, that is, there exists two constants $\underline{\lambda}$ and $\overline{\lambda}$ such that $0 < \underline{\lambda} \le \lambda(k_i) \le \overline{\lambda}$ for all i; (ii) the total number of nodes is constant so that deaths are balanced by births and hence $b = \mu$; (iii) the degree of each node is assumed to be time invariant, that is, the network is static. In reality, the network will be dynamic where new nodes (i.e., born) are added into the network and old nodes are removed (i.e., dead) from the network. However, the adding and removal nodes and edges only take a small proportion in the network and will slightly change the structure of the network. Thus, this is a reasonable simplification (cf. [29]).

For a practical consideration, we will focus on the dynamics of solutions of SIRS system (2.1) in the following bounded region:

$$\Omega := \left\{ \left(S_{k_1}, I_{k_1}, R_{k_1}, \cdots, S_{k_n}, I_{k_n}, R_{k_n} \right) : S_{k_i} \ge 0, I_{k_i} \ge 0, R_{k_i} \ge 0, S_{k_i} + I_{k_i} + R_{k_i} = 1, 1 \le i \le n \right\},$$

and the initial conditions will be given in Ω with $\Theta(0) > 0$. We now establish some properties of solutions of SIRS system (2.1).

Lemma 2.1. Let $\left(S_{k_1}, I_{k_1}, R_{k_1}, \cdots, S_{k_n}, I_{k_n}, R_{k_n}\right)$ be the solution of SIRS system (2.1) with a given initial condition in Ω and $\Theta(0) > 0$. Then for $i = 1, 2, \cdots, n$, we have $0 < S_{k_i}(t) < 1, 0 < I_{k_i}(t) < 1, 0 < R_{k_i}(t) < 1$ and $\Theta(t) > 0$ for all $t > 0$.

One can easily find that the SIRS system (2.1) always has a disease-free equilibrium $\boldsymbol{E}_0 = \left(E_0, E_0, \cdots, E_0\right)^T \in \boldsymbol{F}^n$ with $E_0 = (1,0,0)$ and $\boldsymbol{F} = \boldsymbol{R}^3$. Now, we are going to show that there exists a threshold value R_0, which is related to the parameters in system (2.1) and the network structure, such that if $R_0 > 1$ then another unique endemic equilibrium exists as well. Later in Section 3, we will further prove that the global stability of these two equilibria is indeed completely determined by the threshold value R_0.

Lemma 2.2. Define the value

$$R_0 := \frac{\langle \lambda(k)\varphi(k) \rangle}{(\alpha + \mu)\langle k \rangle}, \tag{2.2}$$

where $\langle \lambda(k)\varphi(k) \rangle := \sum_{i=1}^{n} \lambda(k_i)\varphi(k_i)P(k_i)$. Then the SIRS system (2.1) has a unique endemic equilibrium $\boldsymbol{E}^* = \left(E_1^*, E_2^*, \cdots, E_n^*\right)^T$ if and only if $R_0 > 1$. Here each $E_i^* := \left(S_{k_i}^*, I_{k_i}^*, R_{k_i}^*\right)$, $1 \le i \le n$, satisfies

$$S_{k_i}^* = \frac{\alpha + \mu}{\lambda(k_i)\Theta^*} I_{k_i}^*, \quad I_{k_i}^* = \frac{\lambda(k_i)\Theta^*(\mu + \gamma)}{(\mu + \gamma)(\alpha + \mu + \lambda(k_i)\Theta^*) + \alpha\lambda(k_i)\Theta^*}, \quad R_{k_i}^* = \frac{\alpha}{\mu + \gamma} I_{k_i}^* \tag{2.3}$$

3. Global stability of equilibria

In this section, the global stability of equilibria $\boldsymbol{E}_0$ and $\boldsymbol{E}^*$ will be investigated. We first consider the local asymptotic stability and then the global attractivity of the disease-free equilibrium $\boldsymbol{E}_0$. More specifically, we will show that if the threshold value $R_0 < 1$, then $\boldsymbol{E}_0$ is globally asymptotically stable and if $R_0 = 1$, it is globally attractive. Otherwise, it is unstable. We now state the results of the local stability of $\boldsymbol{E}_0$

Theorem 3.1. The disease-free equilibrium $\boldsymbol{E}_0$ of SIRS system (2.1) is locally asymptotically stable if $R_0 < 1$ and it is unstable if $R_0 > 1$.

Theorem 3.2. If $R_0 < 1$, then the disease-free equilibrium $\boldsymbol{E}_0$ of SIRS system (2.1) is globally asymptotically stable. If $R_0 = 1$, then $\boldsymbol{E}_0$ is globally attractive.

The following result is obtained by constructing a suitable Lyapunov function with the LaSalle's invariant principle [8].

Theorem 3.3. If $R_0 > 1$, then the endemic equilibrium $\boldsymbol{E}^*$ of SIRS system (2.1) is globally asymptotically stable.

4. Numerical experiments

In this section, we will give several numerical examples with various infectivities □(ki) to illustrate the theoretical analysis. The considered network architecture is the scale-free network constructed by means of the preferential attachment algorithm [2]. Later, we will investigate the epidemic dynamics on clustered scale-free networks, namely, consisting of scale-free subnetworks. Some interesting phenomena can be observed in our simulations.

4.1. Global stability of the disease-free equilibrium $\boldsymbol{E}_0$

In this subsection, we give three examples respective corresponding to linear, constant and nonlinear infectivity $\phi(k_i)$ to verify the stability of the disease-free equilibrium $\boldsymbol{E}_0$. The numerical simulations are performed based on a scale-free network with 100 nodes. The scale-free network is constructed in the following manner [2]: it starts with $m_0 = 5$ fully connected nodes, and then each time a new node is added to the network with $m = 2$ links until the network size 100 is reached. In simulation we find that there are 15 different values of degree, i.e., $n = 15$, the minimum degree $k_1 = 2$, the maximum degree $k_{15} = 20$, and the mean degree $\langle k \rangle = 4$. The schematic diagram of the scale-free network with a smaller size 20 is depicted in Figure 1.

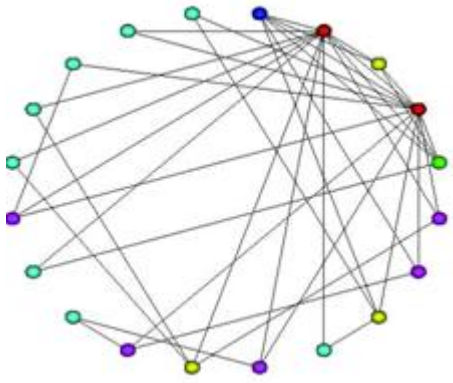

Figure 1. A Barab´asi-Albert scale-free network of 20 nodes with $m_0 = 5$ and $m = 2$

Example 4.1. Let the infection rate $\lambda(k_i) = \lambda k_i$ with $\lambda = 0.01$ and the infectivity $\varphi(k_i) = k_i$ [17]. This leads to $\langle \lambda(k)\varphi(k) \rangle = 0.2972$. Other parameters in system (2.1) are chosen as $\alpha = 0.05$, $b = \mu = 0.05$ and $\gamma = 0.1$. Then one can verify that $R_0 = 0.7430 < 1$. Thus, it follows from

Theorem 3.2 that the disease-free equilibrium $\boldsymbol{E}_0$ is globally asymptotically stable. To illustrate this global property, we measure the error between a given trajectory with $\boldsymbol{E}_0$ by

$$Err(t) := \left\| \left(S_{k_1}(t), I_{k_1}(t), R_{k_1}(t), \cdots, S_{k_n}(t), I_{k_n}(t), R_{k_n}(t) \right)^T - \boldsymbol{E}_0 \right\|_\infty \quad \text{for} \quad t \geq 0 , \tag{4.1}$$

and we use 20 different initial conditions to plot the time evolution of $Err(t)$ in Figure 2(a). As it is seen, for each initial condition, the error curve approaches to zero eventually and so the corresponding solution converges to $\boldsymbol{E}_0$ asymptotically. In addition, the time evolution of the densities of each state for an initial condition are drawn in Figure 2(b), 2(c) and 2(d). One can observe that the disease indeed dies out eventually.

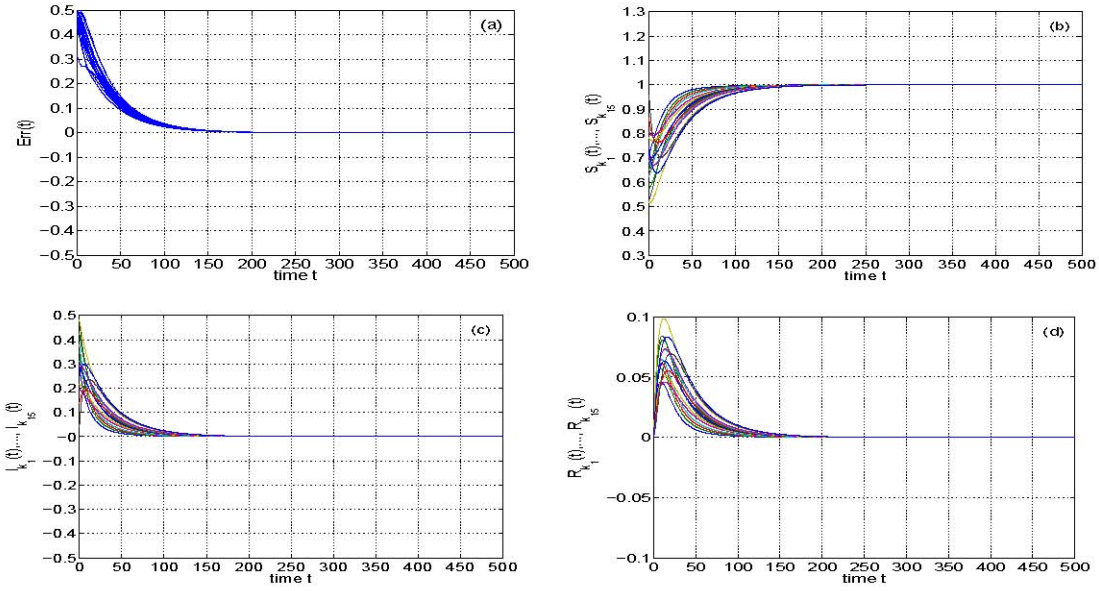

Figure 2. (Example 4.1) (a): The plot of $Err(t)$ for 20 different initial conditions; (b)(c)(d): The time evolution of the densities of each state for an initial condition. The parameters are given by $\lambda(k_i) = 0.01k_i$, $\varphi(k_i) = k_i$, $\alpha = 0.05$, $b = \mu = 0.05$ and $\gamma = 0.1$. The epidemic threshold value is $R_0 = 0.7430$.

Example 4.2. We now consider another system with the same settings as in Example 4.1, except for the infectivity $\varphi(k_i) = C = 2$ (cf. [24]). Then we have $\langle \lambda(k)\varphi(k) \rangle = 0.08$ and we can deduce that $R_0 = 0.2 < 1$. By Theorem 3.2, the disease-free equilibrium $\boldsymbol{E}_0$ is globally asymptotically stable. The plots of $Err(t)$ and the time evolution of the densities of each state are depicted in Figure 3.

Example 4.3. The last example in this subsection is a system with the nonlinear infectivity $\varphi(k_j) = \rho k_j^a / (1 + \nu k_j^a)$ with $\rho = 5$, $\nu = 1$ and $a = 0.5$ [26]. Other parameters are set the same as in Example 4.1. Thus, we have $\langle \lambda(k)\varphi(k) \rangle = 0.1383$ and $R_0 = 0.3457 < 1$. Due to Theorem 3.2

again, the disease-free equilibrium E0 is globally asymptotically stable. The plots of $Err(t)$ and the time evolution of the densities of each state are depicted in Figure 4.

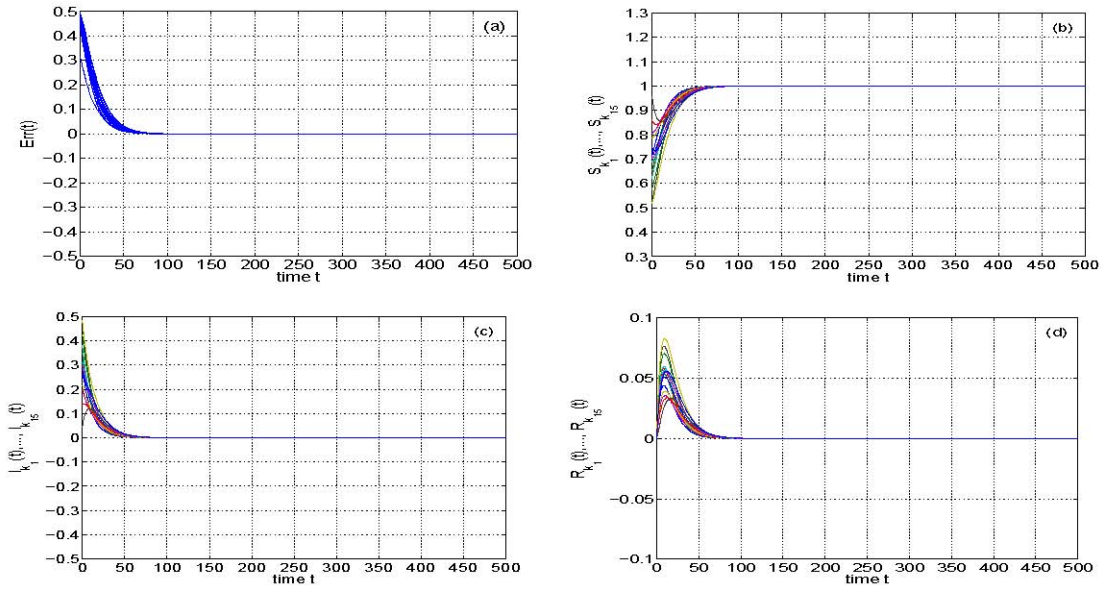

Figure 3. (Example 4.2) (a): The plot of $Err(t)$ for 20 different initial conditions; (b)(c)(d): The time evolution of the densities of each state for an initial condition. The parameters are the same as in Example 4.1 except for $\varphi(k_i)=2$. The epidemic threshold value is $R_0=0.2$.

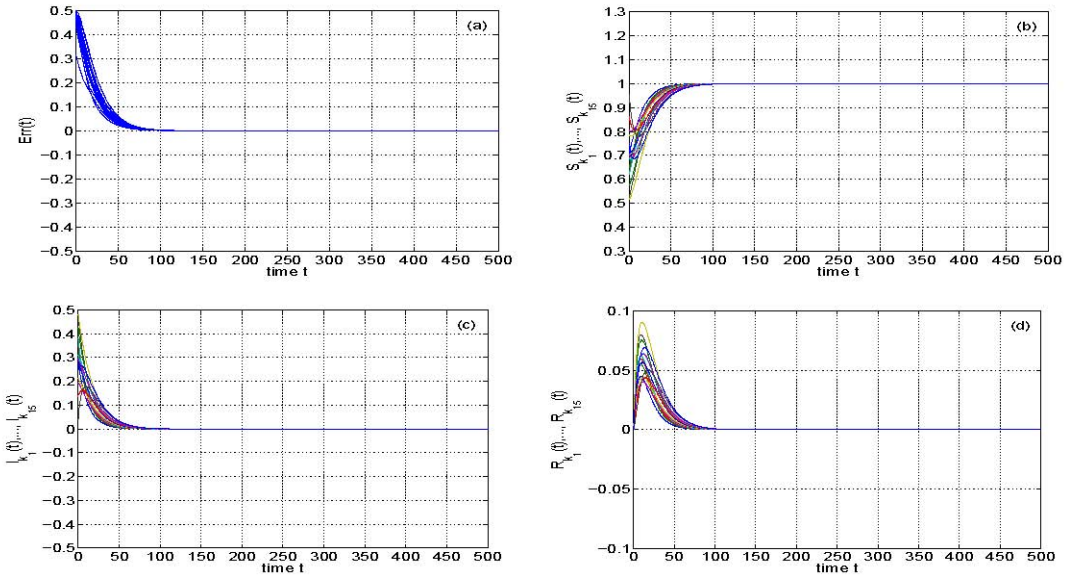

Figure 4. (Example 4.3) (a): The plot of $Err(t)$ for 20 different initial conditions; (b)(c)(d): The time evolution of the densities of each state for an initial condition. The parameters are the same as in Example 4.1 except for $\varphi(k_i)=5\sqrt{k_i}\,/(1+\sqrt{k_i})$. The epidemic threshold value is $R_0=0.3457$.

4.2. Global stability of the endemic equilibrium $\boldsymbol{E}^*$

In this subsection, we turn to verify the global asymptotical stability of the endemic equilibrium $\boldsymbol{E}^*$. The considered network architecture is the same as in Subsection 4.1. Three examples are given to confirm the analysis made in Theorem 3.3.

Example 4.4. In this example, the parameters are chosen the same as in Example 4.1, except for $b = \mu = 0.01$. Then, one can verify that $R_0 = 1.2383 > 1$. Thus, it follows from Theorem 3.3 that the endemic equilibrium $\boldsymbol{E}^*$ is globally asymptotically stable. Similarly, the error plots for 20 different trajectories and the time evolution of the densities of each state for an initial condition are drawn in Figure 5. Here the error measurement is replaced by

$$Err(t) := \left\| \left(S_{k_1}(t), I_{k_1}(t), R_{k_1}(t), \cdots, S_{k_n}(t), I_{k_n}(t), R_{k_n}(t) \right)^T - \boldsymbol{E}^* \right\|_\infty \quad \text{for} \quad t \geq 0, \tag{4.2}$$

From Figure 5, one can see that the densities of each state converge to a positive value for sufficiently large t. This shows that the disease is persistent in the network and approaches an equilibrium state eventually.

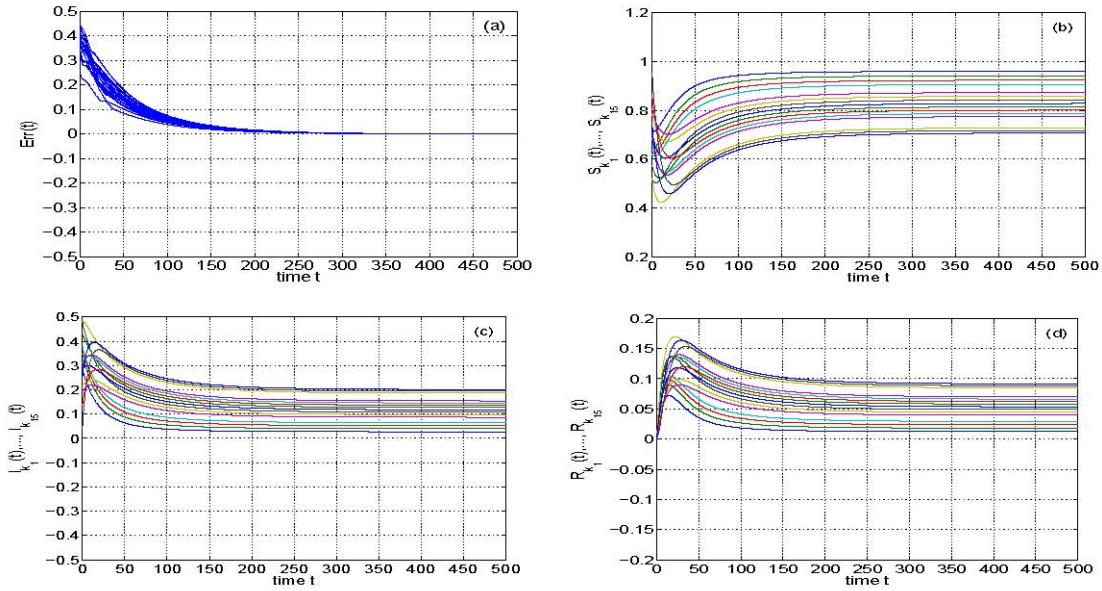

Figure 5. (Example 4.4) (a): The plot of $Err(t)$ for 20 different initial conditions; (b)(c)(d): The time evolution of the densities of each state for an initial condition. The parameters are the same as in Example 4.1, except for $b = \mu = 0.01$. The epidemic threshold value is $R_0 = 1.2383$.

Example 4.5. We now consider another system with the same settings as in Example 4.2, except for $\lambda = 0.05$ and $b = \mu = 0.01$. This implies that $\langle \lambda(k)\varphi(k) \rangle = 0.4$ and we can deduce that $R_0 = 1.6667 > 1$. According to Theorem 3.3, the endemic equilibrium $\boldsymbol{E}^*$ is globally

asymptotically stable. The plots of $Err(t)$ for 20 initial conditions and the time evolution of the densities of each state for an initial condition are depicted in Figure 6.

Example 4.6. The example is set the same as Example 4.3, except for $\rho = 10$ and $b = \mu = 0.01$. Thus, we have $\langle \lambda(k)\varphi(k) \rangle = 0.2776$ and $R_0 = 1.1524 > 1$. It follows from Theorem 3.3 that the endemic equilibrium $\boldsymbol{E}^*$ is globally asymptotically stable. The plots of $Err(t)$ and the time evolution of the densities of each state with the nonlinear infectivity $\varphi(k_i) = 10\sqrt{k_i}/(1+\sqrt{k_i})$ are depicted in Figure 7.

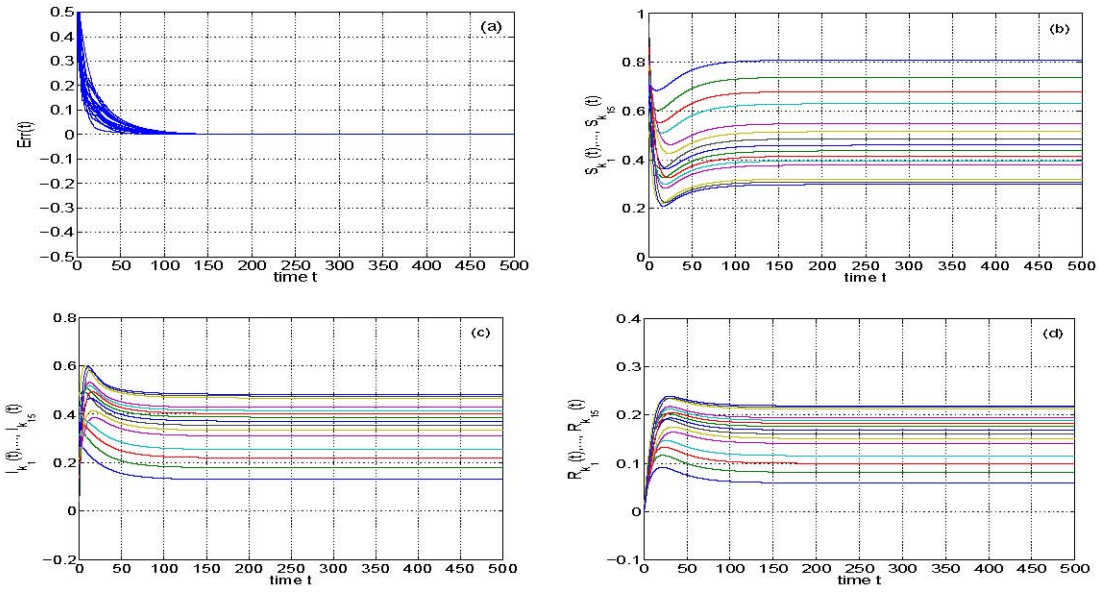

Figure 6. (Example 4.5) (a): The plot of $Err(t)$ for 20 different initial conditions; (b)(c)(d): The time evolution of the densities of each state for an initial condition. The parameters are given by $\lambda = 0.05$ and $b = \mu = 0.01$. The epidemic threshold value is $R_0 = 1.6667$.

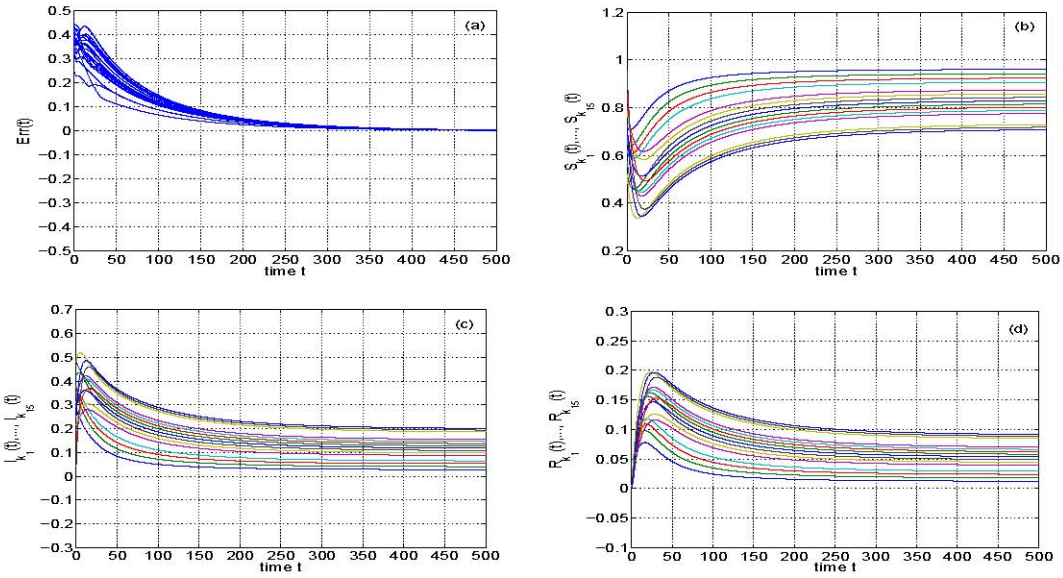

Figure 7. (Example 4.6) (a): The plot of $Err(t)$ for 20 different initial conditions; (b)(c)(d): The time evolution of the densities of each state for an initial condition. The parameters are the same as in Example 4.1 except for $\varphi(k_i)=10\sqrt{k_i}\,/(1+\sqrt{k_i})$ and $b=\mu=0.01$. The epidemic threshold value is $R_0=1.1524$.

4.3. Clustered scale-free networks

So far we have observed the dynamical behavior of various SIRS systems in a single scale-free network. However, the social networks should have some clustered structure (also called community structure). For examining the effect of community structure, it is fundamental to study the epidemic dynamics in clustered networks. In [9], the authors studied how the clustered structure affects epidemic spreading and each cluster in their clustered network is a random subnetwork. Nevertheless, we will study another type of clustered networks, that is, clustered scale-free networks within which each cluster is a scale-free subnetwork. The model of clustered scale-free network is constructed in the following manner: each scale-free subnetwork is generated by the preferential attachment algorithm as we described in Subsection 4.1, namely, it starts with $m_0=5$ fully connected nodes, and then continuously adds a new node with $m=2$ links until a prescribed network size N is reached. This implies that the averaged degree of this subnetwork is $2m$. In fact, the total links within each cluster is mN, so that the probability of intra-cluster links is $p_s=2m/(N-1)$. Assume that there are M such scale-free subnetworks are generated, we use the probability of inter-cluster links p_l to control the links between every two nodes in different clusters. Thus we can define the degree of community $\sigma:=p_s/p_l$ (cf. [9]). We are now in a position to investigate the SIRS dynamics in such a clustered scale-free network.

Example 4.7. This example is devoted to illustrate the case of $R_0<1$. There are 1000 nodes divided

uniformly into 10 clusters. The forms of infection rate $\lambda(k_i)$ and infectivity $\varphi(k_i)$ and other parameters are the same as in Example 4.1. We then define the global average densities of the three epidemic states as follows:

$$S(t)=\sum_{i=1}^{n}P(k_i)S_{k_i}(t)\,,\quad I(t)=\sum_{i=1}^{n}P(k_i)I_{k_i}(t)\,,\quad R(t)=\sum_{i=1}^{n}P(k_i)R_{k_i}(t)$$

In our simulations, for each degree of community, we take 20 configurations and for each configuration, we consider 20 different initial conditions. Thus, we perform 400 realizations to obtain statistically reliable results. The averaged numerical results with various degrees of community are depicted in Figure 8, from which we can see that the disease dies out for all degrees of community. Furthermore, it is shown that the larger the degree of community is, the more rapid convergence to the disease-free steady state will be.

Example 4.8. We now turn to the case of $R_0>1$. As in Example 4.7, we consider 1000 nodesdivided uniformly into 10 clusters. The parameters in SIRS system (2.1) are chosen the same as in Example 4.4. The averaged numerical results with various degrees of community are reported in Figure 9. One can observe from Figure 9 that each state converges to a positive value and so the disease persists for all degree of community. Moreover, we can see that the larger the degree of community is, the stronger the density of susceptible nodes will be, but the weaker the densities of infected and recovered nodes are.

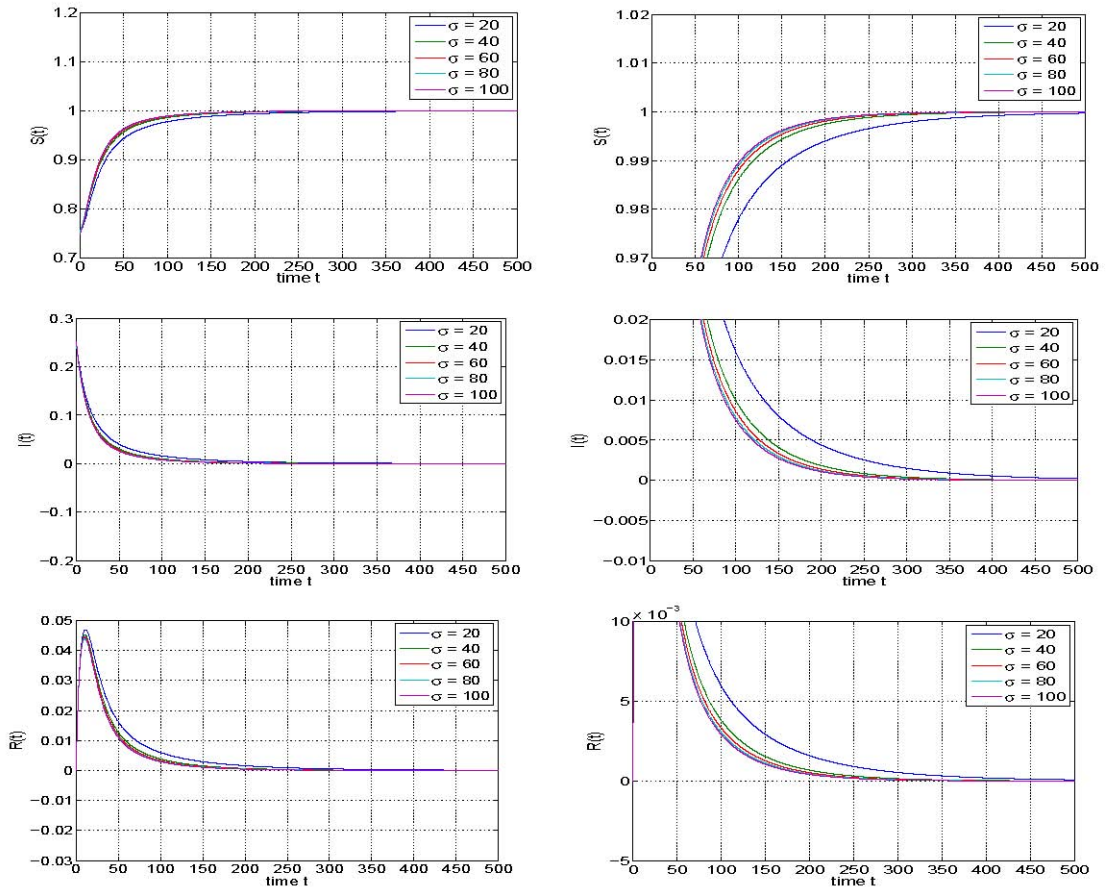

Figure 8. (Example 4.7) Time evolution of the global average densities of each state with different degrees of community, $\sigma = 20,\ 40,\ \cdots,\ 100$. The right column contains local amplifications of the left column.

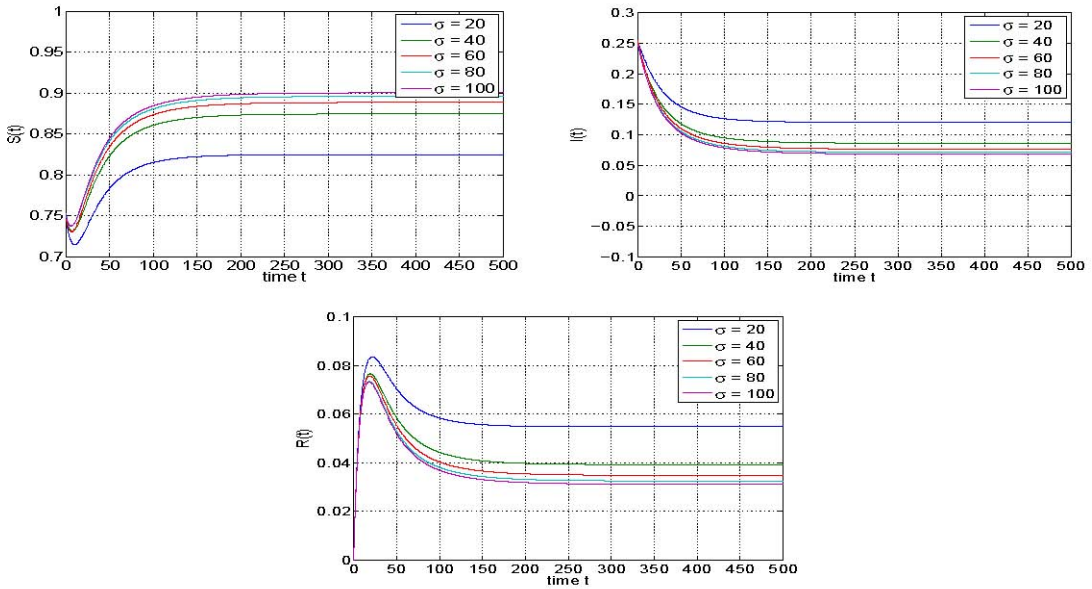

Figure 9. (Example 4.8) Time evolution of the global average densities of each state with different degrees of community, $\sigma = 20,\ 40,\ \cdots,\ 100$.

5. Conclusions and future works

In this paper, we have investigated the epidemic dynamics of an SIRS model with birth and death rates in complex heterogeneous networks. We have proved that there exists a threshold value R_0 which determines not only the existence of the endemic equilibrium $\boldsymbol{E}^*$ but also the global stability of the disease-free equilibrium E0 and the endemic equilibrium $\boldsymbol{E}^*$. More specifically, we have proved that if $R_0 < 1$ then $\boldsymbol{E}_0$ is globally asymptotically stable, and as $R_0 = 1$, $\boldsymbol{E}_0$ is globally attractive. This indicates that if $R_0 \le 1$ and there are infected nodes at the initial time, the disease always dies out. On the other hand, if $R_0 > 1$ then the disease-free equilibrium $\boldsymbol{E}_0$ becomes unstable and in the meantime, there exists uniquely an endemic equilibrium $\boldsymbol{E}^*$ which is globally asymptotically stable. This means that if $R_0 > 1$ and there are infected nodes at the initial time, the disease will be persistent in the network and it will approach a positive equilibrium state eventually.

We have also performed a series of numerical experiments to confirm the correctness of the theoretical analysis. In addition, for examining the effect of community structure of the complex heterogeneous networks on the epidemic dynamics, we have considered the epidemic spreading in the clustered scale-free networks. We have found that for the convergence of the disease-free steady state, with the increase of the degree of community, the convergent rate to the disease-free equilibrium will be increased. On the other hand, for the convergence of endemic steady state, the larger the degree of community is, the stronger the density of susceptible nodes will be, but the weaker the densities of infected and recovered nodes are.

Finally, we conclude this paper with the following remark. From the threshold value R_0 given in (2.2), one can find that it is dependent on the infectivities $\varphi(k_i)$, the infection rates through each edge $\lambda(k_i)$ and the mean degree $\langle k \rangle$ of the considered network. In other words, the network topology will affect the value of R_0. Consequently, how to control the epidemic spreading by changing the topology of the complex heterogeneous network will be a fundamental issue. This effort is in progress and we will report the results in the near future.

References

[1] R. M. Anderson and R. M. May, Infectious Diseases in Humans: Dynamics and Control, Oxford University Press, Oxford, 1992.

[2] A.-L. Barab´asi and R. Albert, Emergence of scaling in random networks, Science, 286 (1999),

pp. 509-512.

[3] S. Bansal, B. T. Grenfell, and L. A. Meyers, When individual behaviour matters: homogeneous and network models in epidemiology, J. R. Soc. Interface, 4 (2007), pp. 879-891.

[4] X. Fu, M. Small, D. M. Walker, and H. Zhang, Epidemic dynamics on scale-free networks with piecewise linear infectivity and immunization, Phys. Rev. E, 77 (2008), 036113.

[5] H. W. Hethcote, The mathematics of infectious diseases, SIAM Rev., 42 (2000), pp. 599-653.

[6] J. Joo and J. L. Lebowitz, Behavior of susceptible-infected-susceptible epidemics on heterogeneous networks with saturation, Phys. Rev. E, 69 (2004), 066105.

[7] A. Korobeinikov and G. C. Wake, Lyapunov functions and global stability for SIR, SIRS, and SIS epidemiological models, Appl. Math. Lett., 15 (2002), pp. 955-960.

[8] J. P. LaSalle, The Stability of Dynamical Systems, SIAM, Philadelphia, PA, 1976.

[9] Z. Liu and B. Hu, Epidemic spreading in community networks, Europhys. Lett., 72 (2005), pp. 315-321.

[10] J. Liu and T. Zhang, Epidemic spreading of an SEIRS model in scale-free networks, Commun. Nonlinear Sci. Numer. Simul., 16 (2011), pp. 3375-3384.

[11] I. A. Moneim, Seasonally varying epidemics with and without latent period: a comparative simulation study, Math. Med. Biol., 24 (2007), pp. 1-15.

[12] Y. Moreno, R. Pastor-Satorras, and A. Vespignani, Epidemic outbreaks in complex heterogeneous networks, Eur. Phys. J. B, 26 (2002), pp. 521-529.

[13] M. E. J. Newman and M. Girvan, Finding and evaluating community structure in networks, Phys. Rev. E, 69 (2004), 026113.

[14] M. E. J. Newman and J. Park, Why social networks are different from other types of networks, Phys. Rev. E, 68 (2003), 036122.

[15] R. Olinky and L. Stone, Unexpected epidemic thresholds in heterogeneous networks: The role of disease transmission, Phys. Rev. E, 70 (2004), 030902(R).

[16] A. d'Onofrio, A note on the global behaviour of the network-based SIS epidemic model, Nonlinear Anal.-Real World Appl., 9 (2008), pp. 1567-1572.

[17] R. Pastor-Satorras and A. Vespignani, Epidemic dynamics in scale-free networks, Phys. Rev. Lett., 86 (2001), 3200.

[18] R. Pastor-Satorras and A. Vespignani, Epidemic dynamics in finite size scale-free networks, Phys. Rev. E, 65 (2002), 035108(R).

[19] M. Small and C. K. Tse, Clustering model for transmission of the SARS virus: application to epidemic control and risk assessment, Physica A, 351 (2005), pp. 499-511.

[20] L. Wang and G.-Z. Dai, Global stability of virus spreading in complex heterogeneous networks, SIAM J. Appl. Math., 68 (2008), pp. 1495-1502.

[21] Q.-C. Wu, X.-C. Fu, and M. Yang, Epidemic thresholds in a heterogenous population with competing strains, Chin. Phys. B, 20 (2011), 046401.

[22] Y. Xiao, Y. Zhou, and S. Tang, Modelling disease spread in dispersal networks at two levels, Math. Med. Biol., 28 (2011), pp. 227-244.

[23] M. Yang, G. Chen, and X. Fu, A modified SIS model with an infective medium on complex networks and its global stability, Physica A, 390 (2011), pp. 2408-2413.

[24] R. Yang, B.-H. Wang, J. Ren, W.-J. Bai, Z.-W. Shi, W.-X. Wang, and T. Zhou, Epidemic spreading on heterogeneous networks with identical infectivity, Phys. Lett. A, 364 (2007), pp. 189-193.

[25] M. Youssef and C. Scoglio, An individual-based approach to SIR epidemics in contact networks, J. Theor. Biol., 283 (2011), pp. 136-144.

[26] H. Zhang and X. Fu, Spreading of epidemics on scale-free networks with nonlinear infectivity, Nonlinear Anal.-Theory Methods Appl., 70 (2009), pp. 3273-3278.

[27] J.-P. Zhang and Z. Jin, The analysis of an epidemic model on networks, Appl. Math. Comput., 217 (2011), pp. 7053-7064.

[28] J.-P. Zhang and Z. Jin, Epidemic spreading on complex networks with community structure, Appl. Math. Comput., 219 (2012), pp. 2829-2838.

[29] G. Zhu, X. Fu, and G. Chen, Global attractivity of a network-based epidemic SIS model with nonlinear infectivity, Commun. Nonlinear Sci. Numer. Simul., 17 (2012), pp. 2588-2594.

[30] G. Zhu, X. Fu, and G. Chen, Spreading dynamics and global stability of a generalized epidemic model on complex heterogeneous networks, Appl. Math. Model., 36 (2012), pp. 5808-5817.